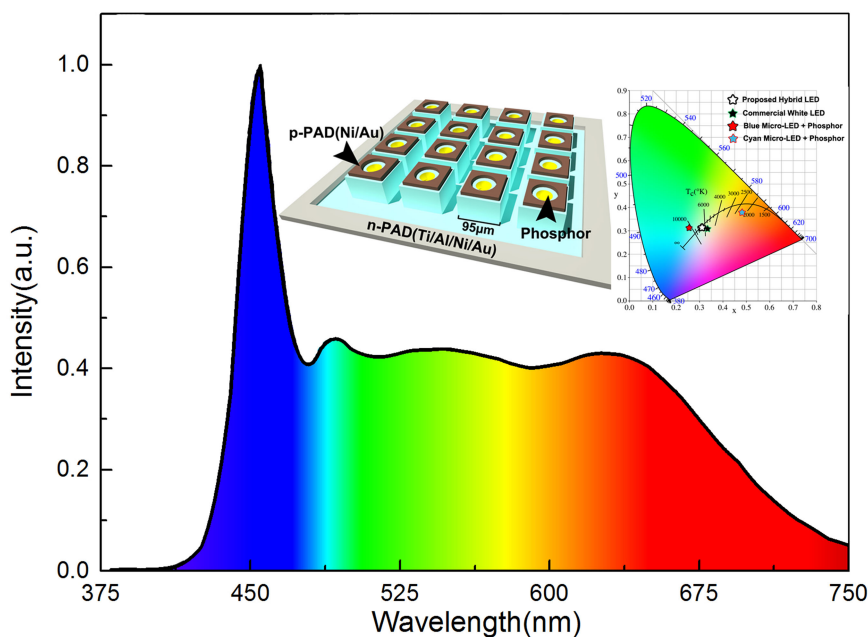


Hybrid Cyan Nitride/Red Phosphors White Light-Emitting Diodes With Micro-Hole Structures

Volume 10, Number 5, September 2018

Tao Tao
Ting Zhi
Xu Cen
Bin Liu
Qi Wang
Zili Xie
Peng Chen
Dunjun Chen
Yugang Zhou
Youdou Zheng
Rong Zhang



Hybrid Cyan Nitride/Red Phosphors White Light-Emitting Diodes With Micro-Hole Structures

Tao Tao,^{1,2} Ting Zhi,³ Xu Cen,^{1,2} Bin Liu^{1,2}, Qi Wang,^{1,2} Zili Xie,^{1,2}
Peng Chen^{1,2}, Dunjun Chen,^{1,2} Yugang Zhou^{1,2},
Youdou Zheng,^{1,2} and Rong Zhang^{1,2}

¹Jiangsu Provincial Key Laboratory of Advanced Photonic and Electronic Materials, School of Electronic Science and Engineering, Nanjing University, Nanjing 210093, China

²Nanjing National Laboratory of Microstructures, Nanjing University, Nanjing 210093, China

³College of Electronic and Optical Engineering and College of Microelectronics, Nanjing University of Posts and Telecommunications, Nanjing 210093, China

DOI:10.1109/JPHOT.2018.2872035

1943-0655 © 2018 IEEE. Translations and content mining are permitted for academic research only.

Personal use is also permitted, but republication/redistribution requires IEEE permission.

See http://www.ieee.org/publications_standards/publications/rights/index.html for more information.

Manuscript received August 31, 2018; revised September 19, 2018; accepted September 20, 2018. Date of publication September 24, 2018; date of current version October 9, 2018. This work was supported in part by the National Key Research and Development Program of China under Grant 2016YFB0400602 and Grant 2017YFB0403101, in part by the National Nature Science Foundation of China under Grant 61605071, Grant 61674076, Grant 61274003, Grant 61422401, Grant 51461135002, and Grant 61334009, in part by Nature Science Foundation of Jiangsu Province under Grant BY2013077, Grant BK20141320, and Grant BE2015111, in part by Fundamental Research Funds for the Central Universities under Grant 021014380096 and Grant 021014380104, in part by Collaborative Innovation Center of Solid State Lighting and Energy-Saving Electronics, in part by Six Talent Peaks Project of Jiangsu Province (XYDXX-081), in part by Open Fund of the State Key Laboratory on Integrated Optoelectronics (IOSKL2017KF03), and in part by the Research Funds from NJU-Yangzhou Institute of Opto-Electronics. Corresponding authors: T. Tao and B. Liu (e-mail: ttao@nju.edu.cn; bliu@nju.edu.cn).

Abstract: Hybrid white light emitting diodes (LEDs) have been developed utilizing micro-LEDs radiatively pumping down-conversion phosphor materials. The cyan InGaN/GaN multiple quantum wells LEDs with 95 μm in square are fabricated into 4×4 pixels as one unit in 4 in wafer by photolithography and inductively coupled plasma etching techniques. The relatively low turn ON voltage and low leakage of cyan micro-LEDs indicate good electrical performance. A significant reduction in the efficiency droop characteristics of cyan micro-LED has been observed in comparison with that of standard green LED. Finally, based on a systemic optimization for white emission indexes, high-quality hybrid white light emission has been demonstrated by the combination of blue and cyan micro-LEDs with two types of phosphors, which have a high color rendering index up to 87 at the correlated color temperatures of 6500 K. It also demonstrates a way to adjust the color component by modifying the output power of cyan micro-LED in hybrid LED, showing a promising candidate in a large range of applications including micro-displays, bioinstrumentation, photolithography, and lab-on-chip systems in the future.

Index Terms: —.

1. Introduction

The need has been emphasized for efficient solid-state emitters in wide applications ranging from displays to luminescence lighting because they potentially provide substantial energy savings to

allow for efficient energy utilization of limited energy resources [1]. The conventional approach is to mainly use blue emission from InGaN/GaN-based light emitting diodes (LEDs) radiatively pumping down-conversion phosphor materials, such as $\text{Y}_3\text{Al}_5\text{O}_{12}:\text{Ge}^{3+}$ (YAG), to provide artificial white lighting [2], [3]. During the past decade, much works have been devoted to the development of InGaN-based solid-state lighting using the “blue LED + yellow phosphor” [4], [5]. However, these white LEDs have low color rendering index (CRI) and high correlated color temperature (CCT) owing to green emission deficiency in the visible spectrum [2]. Micro-LEDs within cyan or green emission range are highly required, which have acquired increasing world-wide interest recently [6]. Moreover, these phosphors spun on the p-GaN of blue LED with the distance of above 200 nm between the phosphors and the emitter (multiple quantum wells), which induce other issues such as the self-absorption of the phosphors, the low efficiency of energy transfer from the blue LED to the down-conversion phosphor and the degradation of phosphors. For the sake of reducing the coupling distance, Zhuang *et al.* developed CdSe/ZnS core/shell nano-crystals filling the ordered arrays of nanoholes technique, and achieved white LEDs with high color rendering index (CRI) up to 82. However, the green gap issues still require consideration and further developments for the high CRI of white LEDs in the visible spectrum [7].

In order to extend the functionality of GaN-based LED to advanced applications including image display, visible light communications, optical tweezers, optogenetics, and maskless lithography, scientists started to devote their efforts to developing the high power and high efficiency III-nitride based LEDs [8]. Most efforts have concentrated on the improvement of material quality, internal quantum efficiency (IQE) and light extraction efficiency [9]. Especially, for the sake of acquiring high luminescence output power, the standard GaN-based LED light emitting areas are normally defined as large as a few square millimeters. Although, these high power white LEDs with large device size are currently massively used for solid-state lighting and liquid crystal display back-lighting area, the large device size limits the development of high resolution for image display [10]. The needs of micro-LEDs with individual color, especially in the green gap emission range where GaN-based LEDs have low efficiency, are growing rapidly [6], [11]. In comparison with standard LEDs, micro-pixelated LEDs with individual pixel only a few tens of square micrometers are able to offer greater contrast, faster response time and less energy consumption, therefore are currently the main approach toward a fast growing market [12]. However, micro-LEDs are still in their early development stage compared with the conventional LEDs fabrication technology. The mesa-etching method of defining pixel introduce tense defects, which becomes more problematic as the ratio of sidewall area to pixel area increases in micro-LEDs. Moreover, there is still no cost-effective fabrication technology for green or cyan inorganic micro-LED to fill the green gap in full-color display and white luminescence. And the competition between organic and inorganic micro-LEDs approaches is intense at this stage [13], especially the related study on GaN-based micro-LEDs is quite limited. Thus, white micro-LEDs with high efficiency and CRI have acquired increasing world-wide interest recently.

In this work, a high color rendering index hybrid GaN-based white micro-LED array is designed and fabricated. Current-voltage (*I-V*) characterizations of the white micro-LED pixels with cyan emitters are conducted and analyzed. A significant reduction in the efficiency droop characteristics of cyan micro-LED has been observed in comparison with that of standard green LED. Hybrid white light emission has been demonstrated by the combination of blue and cyan micro-LEDs with phosphors, which have a high color rendering index up to 87 at the correlated color temperatures of 6500 K. It offers a promising method for practical applications including high quality and resolution image display and visible light communications.

2. Results and Discussion

Figure 1(a) presents the schematic of the designed cyan micro-LED, showing that the sharing common cathode are fabricated on a planar GaN-based LED epi-wafer. The epi-structure is grown on a 4-inch sapphire substrate by using metal-organic chemical vapor deposition (MOCVD) with a relatively small wafer bow ($<80 \mu\text{m}$), which consists of 3 μm undoped GaN buffer layer, a 2 μm

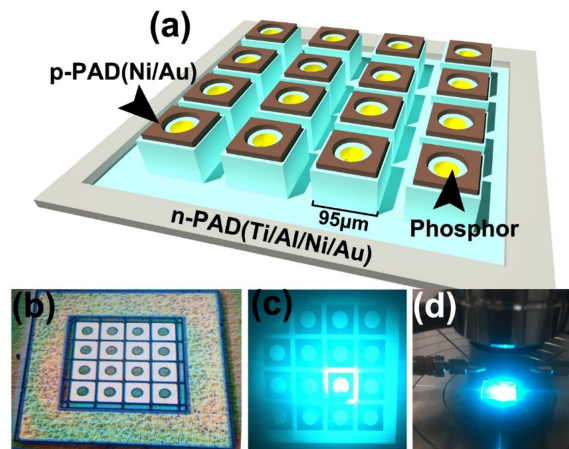


Fig. 1. (a) Schematic diagrams of cyan micro-LED array with 4×4 pixels. (b) Bird's eye view microscope image of cyan micro-LED. (c) CCD image of one pixel in cyan micro-LED array at the injection current of $200 \mu\text{A}$. (d) The picture of cyan micro-LED emission at the injection current of $200 \mu\text{A}$.

Si doped n-type GaN layer, a 15 period InGa_xN/GaN (3 nm/12 nm) multi-quantum wells (MQWs), a 60-nm-thin AlGa_xN electron blocking layer, and a 270 nm Mg doped p-type GaN layer. The In content in In_xGa_{1-x}N layer of MQWs is designed and grown to be about 0.21 for the sake of cyan light emission. The surface roughness of our fabricated 4-inch cyan wafer is about 2.1 nm within $20 \mu\text{m} \times 20 \mu\text{m}$ square area. $300 \mu\text{m} \times 300 \mu\text{m}$ square mesa was etched in standard LED samples for references. The micro-LED pixels are fabricated by a similar process for flip-chip LEDs, which starts with mesa etching. As illustrated in Fig. 1(a), $95 \mu\text{m} \times 95 \mu\text{m}$ square pixel area is defined by photolithography and inductively coupled plasma (ICP) etching techniques. Next, the devices are passivated by a 200-nm-thick SiO₂ layer deposited by plasma enhanced chemical vapor deposition (PECVD) after the wet chemical surface treatments involving the utilizing of hot potassium hydroxide (KOH) and nitric acid (HNO₃). The metal contact window opening is chemically etched by reactive-ion etching (RIE) processes. Finally, n-type (Ti:50 nm/Al:200 nm/Ni:50 nm/Au:100 nm) metal contact layer are deposited on n-pad region and annealed at 760 °C in nitrogen atmosphere for 10 min. And then p-type (Ni:10 nm/Au:200 nm) metal contact layer are deposited on p-pads regions and annealed at 560 °C in mixed atmosphere (80% nitrogen and 20% oxygen) for 3 min to form Ohmic contacts. Each unit consists of 4×4 pixels arrayed in orthogonal configuration. Each pixel is separated by $5 \mu\text{m}$ wide deep trench to constrain the light emitting region. All pixels have independent p-type contact pads, which expose circular region with $40 \mu\text{m}$ in diameter for the light emitting and color conversion by phosphors or semiconductor nano-crystals. A large size cathode electrode is made surrounding the array area to ensure efficient and uniform n-type current injection for all micro-LED pixels in array. In future massive transfer processes, cathode electrode pads can be adjusted to backside or individual contact for single pixel based on the demands of chip packaging or image display. Fig. 1(b) illustrates the bird's eye top-view image of one cyan micro-LED array. Fig. 1(c) and (d) demonstrate the cyan light emitting image from single micro-LED pixel. The emission of single cyan micro-LED pixel is greatly bright and uniform under the injection current of $200 \mu\text{A}$.

Room temperature photoluminescence (PL) spectra of cyan epi-wafer was firstly gathered using a Renishaw InVia Micro-PL system equipped with a $40 \times$ UV objective lens (Mitutoyo, numerical aperture = 0.5). As shown in Fig. 2(a), the dominant PL peak locates at 482 nm with full width at half maximum (FWHM) about 23.2 nm. The experimental (0002) X-ray diffraction for cyan epi-wafer sample were scanned by PANalytical X'Pert Pro MRD triple-axis X-ray diffraction. As illustrated in Fig. 2(b), several satellite peaks of InGa_xN/GaN MQWs can be seen, indicating a good crystal quality. Through simulation, the thickness of GaN barrier is estimated to be about 11.7 nm, and the

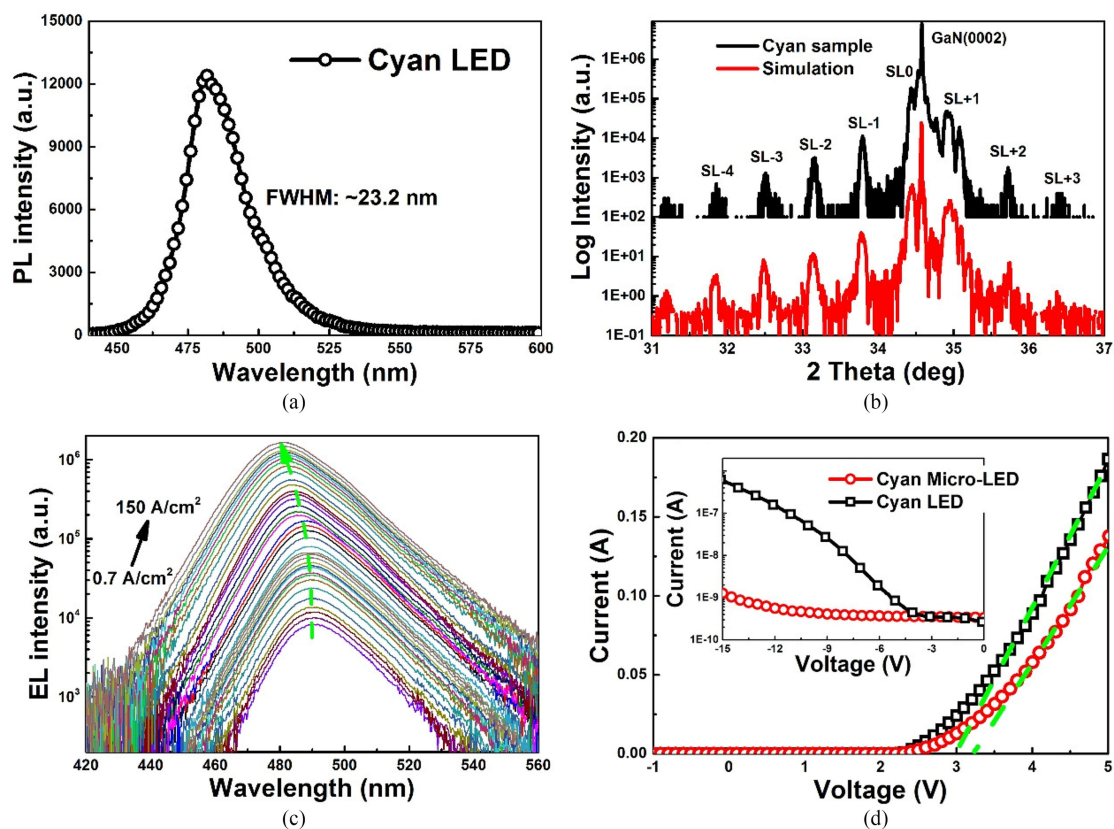


Fig. 2. (a) The PL spectra of cyan epi-wafer. (b) Experimental (black) and simulated (red) (0002) X-ray diffraction scans for cyan epi-wafer grown on sapphire substrate. (c) The EL spectra of one pixel in the cyan micro-LED at the injection current density ranging from 0.7 A/cm^2 to 150 A/cm^2 . (d) I - V characteristics of one pixel in the cyan micro-LED. The inset is the leakage I - V curve in semi-log scale.

InGaN well in MQWs is estimated to be 2.5 nm [14]. The In content x in $\text{In}_x\text{Ga}_{1-x}\text{N}$ layer of MQWs is calculated to be 0.21 , which is consistent with our design. Room temperature electroluminescence (EL) spectra of cyan micro-LED pixel was measured at the injection current ranging from 0.7 A/cm^2 to 150 A/cm^2 . The dominant emission peak of cyan micro-LED blueshifts from the wavelength of 490 nm to about 482 nm with the increasing injection current density, which is mainly attributed to the screening of quantum confined Stark effect (QCSE) caused by increased carrier density in MQWs region. In addition, the current-voltage (I - V) characterizations of the cyan micro-LED pixel and standard LEDs are also conducted as shown in Fig. 2(b), and the corresponding leakage current are plotted on semi-log scale in the inset of the Fig. 2(b). The turn-on voltage of cyan micro-LED is estimated to be around 3.1 V , close to that of standard planar LED [15], which of course still needs further optimization. A low magnitude of electrical leakage current of cyan micro-LED, $1.5 \times 10^{-9} \text{ A}$ under the reverse bias of -15 V , is visible in the reverse I - V characteristics in the inset of Fig. 2(b). Meanwhile, the leakage current of cyan standard LED is $6 \times 10^{-7} \text{ A}$ under the same reverse bias, which is 3 orders of magnitude larger than that of micro-LED. The leakage current density of cyan micro-LED is about two orders of magnitude lower than that of standard LED if the size of emission area are taken into consideration. The good electrical characteristics of micro-LED indicate the importance of the optimization in the electrodes annealing process [16]. We believe the reduction in leakage current of micro-LED is mainly attributed to the increased series resistance and the reduced leakage tunnels such as dislocations and defects by decreasing the device size. Typically, the I - V characteristics of a p-n junction diode are represented by the well-known Shockley diode equation [17], $I = I_0 \exp(eV/nkT)$, where I_0 , e , k , n and T are

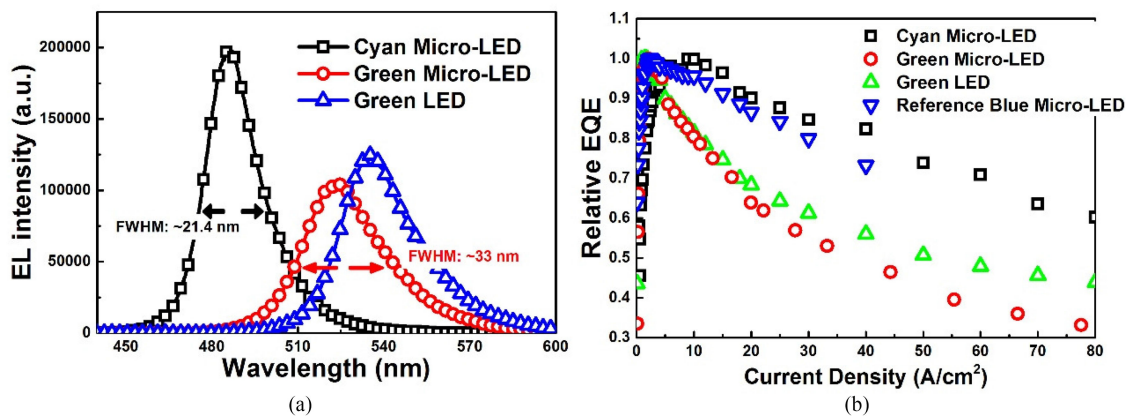


Fig. 3. (a) The EL spectra of cyan micro-LED pixels, standard planar green LED and green micro-LED pixels under the injection current of $900 \mu\text{A}$. (b) Normalized external quantum efficiency of one pixel in cyan micro-LEDs, standard green LEDs, green micro-LED and reference blue micro-LED as a function of the injection current density.

the saturation current, elementary charge, Boltzmann constant, ideality factor and temperature, respectively. It has been widely accepted that, if n is close to 2.0, the generation-recombination current dominates; if n approaches 1.0, diffusion current dominates; whereas if the ideality factor $1 < n < 2$, a combination of diffusion in the quasi-neutral and recombination in the space-charge regions is observed. For the cyan micro-LED, a value of the ideality factor $n = 4$ below the turn on voltage can be derived. It suggests leakage currents associate with carrier recombination in the depletion region via deep-level traps such as dislocation defects, and therefore cause the ideality factor to exceed 2.0. Considering the high ratio of sidewall area to pixel area and low leakage current as mentioned before, the better device performance of cyan micro-LED can be expected, which of course needs further works.

The luminous flux of standard cyan LED is measured to be 3.0533 lm under the injection current of 20 mA using UV-VIS-near IR spectro-photocolorimeter with an integrating sphere (PMS-50). To further explore the optical and electrical performance of the cyan micro-LEDs, the EL emission of cyan micro-LED pixels, standard planar green LED and green micro-LED pixels are measured and compared under the same injection current of $900 \mu\text{A}$. As illustrated in Fig. 3(a), the emission intensity of cyan micro-LED pixel is higher than that of green micro-LED pixel under the same injection current. The FWHM of cyan micro-LED is 21.4 nm, while the FWHM of green micro-LED is 33 nm. The higher EL intensity and lower FWHM indicate a good device performance of cyan micro-LED. The light emitting performance of the cyan micro-LED pixel with respect to standard green LED, green micro-LED and micro-LED in reference under different injection current density is further studied [18]–[20]. A typical efficiency droop behavior of samples in this study are observed from the normalized relative external quantum efficiency (EQE) as a function of the injection current density and are compared with other micro-LEDs reported in references as shown in Fig. 3(b). Normally, the EQE of GaN-based LED gradually drop at higher injection current density after reaching the maximum, revealing a typical efficiency droop behavior. It has been widely reported that efficiency droop in GaN-based LEDs is mainly attributed to non-radiative recombination, electron overflow, and thermal accumulation as the injection current increases [21]. In addition, the lack of holes injection, carrier delocalization, and Auger recombination are also suggested as possible reasons for efficiency droop [22]. From Fig. 3(b), we can see that the green LED and the micro-LED using green chips show similar efficiency droop curves. Meanwhile the cyan micro-LED in this study and blue micro-LED reported in reference exhibit much less efficiency droop at the higher injection current. The maximum EQE point of cyan micro-LED occurs at $\sim 10 \text{ A/cm}^2$, which is higher than that of green LED at 1.5 A/cm^2 . Besides, the EQE of cyan

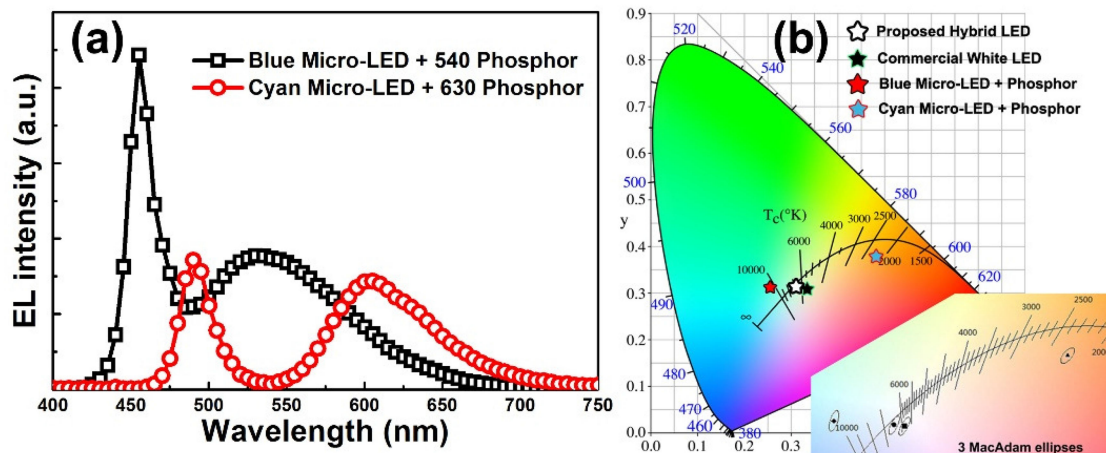


Fig. 4. (a) The EL spectra of blue micro-LED with 540 phosphor and cyan micro-LED with 630 phosphor at the injection current of $500 \mu\text{A}$. (b) The locations of blue and cyan micro-LEDs with phosphors, commercial white LED and proposed hybrid LED in the CIE 1931 chromaticity diagram. Inset: MacAdam ellipses of four samples.

micro-LED pixel drops more slowly than that of green LED at higher current density ($> 1.5 \text{ A/cm}^2$), even a bit slower than that of the blue micro-LED, which further indicates the good performance of cyan micro-LEDs. In this study, cyan LED epi-wafer with less indium incorporation than green LED will certainly reduce the strain accumulated in MQWs region during the growth, thus has lower defect density and less non-radiative recombination centers. It is reasonable to believe that the cyan micro-LED should have better device performance than green LED. Furthermore, the smaller chip size could certainly benefit current spreading and heat dissipation [23]. Low leakage current will reduce the thermal accumulation. And larger height-to-width aspect ratio of micro-LEDs would possibly provide better strain relaxation within the MQWs region. It is interesting that the cyan micro-LEDs illustrate comparable efficiency droop characteristics with respect to blue micro-LED. It indicates much improved growth technique using MOCVD as well as optimized fabrication process. Therefore, the cyan micro-LEDs with good device performance could provide a promising solution for the green gap problem in high quality luminescence and high resolution image display instead of green LED.

Typically, due to the high internal quantum efficiency as much as 80% of GaN-based blue LEDs, the commercial white LED is mainly using GaN-based blue LED with one or two types of phosphors, however, inducing a great green gap at the wavelength of 500 nm in emission spectra. The black square line in Fig. 4(a) exhibits the EL spectra of the blue micro-LEDs with phosphor at the wavelength of 540 nm under the injection current of $500 \mu\text{A}$. The EL spectra have a strong emission peak at the wavelength of 460 nm, with a broad emission ranging from 500 nm to 590 nm. As shown in Fig. 4(a), there is a green gap at the wavelength of around 490 nm, where the emission peak of cyan micro-LED locates. The introduction of cyan micro-LEDs is capable to fill the green gap of commercial white LED. In this work, we propose an idea of hybrid LEDs using blue and cyan micro-LEDs with two types of phosphors to provide high quality illumination project. As demonstrated before, the blue and cyan micro-LEDs are scaled down to less than $100 \mu\text{m}$ in square. In the 1931 CIE chromaticity diagram in Fig. 4(b), the blue micro-LED with 540 nm phosphor locates at (0.261, 0.315) marked by red star. And the cyan micro-LED with 630 nm phosphor locates at (0.482, 0.386) marked by cyan star. Thus, blue and cyan micro-LEDs were used as light emitting sources, where two types of phosphors (540 nm and 630 nm) were filled into exposed circular area in each pixel of micro-LEDs for the light color conversion. Through transfer technique, which is not demonstrated in this article, those micro-LEDs can be put together with individual controlling circuit. Manipulating the input power of blue and cyan micro-LEDs, the CRI and CCT is adjusted, indicating that the

hybrid LED is accessed to change the CCT for various applications. Thus, the proposed hybrid LEDs are labelled by white stars in the 1931 CIE chromaticity diagram in Fig. 4(b). The commercial white LED using phosphors has a CRI of 81 with $T_c = 5000$ K, which is located at (0.332, 0.316) in the 1931 CIE chromaticity diagram labeled as black star, whereas the proposed hybrid LED has a CRI of 87 with $T_c = 6500$ K, located at (0.315, 0.319) in Fig. 4(b), respectively. In addition, the chromaticity coordinates of hybrid LED is much closer to the blackbody line. The combination of blue and cyan micro-LEDs with phosphors offer a powerful method to adjust the color component by modifying the luminescence power of each LED, respectively. High quality image display with high resolution can be expected in the future using the combination of micro-LEDs with different colors, which of course needs further works.

3. Conclusions

In summary, cyan micro-LEDs have been successfully fabricated by a similar process for commercial LEDs. The electrical properties of cyan micro-LEDs are analyzed. The low leakage current, compared to that of standard LED, indicate good electrical performance of our fabricated LEDs. The efficiency droop characteristics of cyan micro-LEDs are studied, which shows much reduced droop behavior compared to those of standard green LED and green micro-LED. High quality hybrid white light emission has been demonstrated by the combination of blue and cyan micro-LEDs with phosphors. We anticipate that the cyan micro-LED with better device performance will be useful in solving the green gap problem of white LED. The hybrid LED also indicates a method to adjust the color component by modifying the output power of each LED, showing a promising candidate in large range of applications including micro-displays, bioinstrumentation, photolithography and lab-on-chip systems in the future.

4. Competing Financial Interests

The authors declare no competing financial interest.

References

- [1] M. Achermann, M. A. Petruska, S. Kos, D. L. Smith, D. D. Koleske, and V. I. Klimov, "Energy-transfer pumping of semiconductor nanocrystals using an epitaxial quantum well," *Nature*, vol. 429, pp. 642–646, 2004.
- [2] W.-R. Liu *et al.*, "(Ba,Sr)Y₂Si₂Al₂O₂N₅: Eu²⁺: A novel near-ultraviolet converting green phosphor for white light-emitting diodes," *J. Mater. Chem.*, vol. 21, pp. 3740–3744, 2011.
- [3] H. P. T. Nguyen *et al.*, "Controlling electron overflow in phosphor-free InGaN/GaN nanowire white light-emitting diodes," *Nano Lett.*, vol. 12, pp. 1317–1323, 2012.
- [4] X. Rong-Jun and H. Naoto, "Silicon-based oxynitride and nitride phosphors for white LEDs—A review," *Sci. Technol. Adv. Mater.*, vol. 8, pp. 588–600, 2007.
- [5] J. Cho, J. Hyuk Park, J. K. Kim, and E. Fred Schubert, "White light-emitting diodes: History, progress, and future," *Laser Photon. Rev.*, vol. 11, 2017, Art. no. 1600147.
- [6] H.-W. Chen, J.-H. Lee, B.-Y. Lin, S. Chen, and S.-T. Wu, "Liquid crystal display and organic light-emitting diode display: Present status and future perspectives," *Light, Sci. Appl.*, vol. 7, 2018, Art. no. 17168.
- [7] Z. Zhuang *et al.*, "High color rendering index hybrid III-Nitride/Nanocrystals white light-emitting diodes," *Adv. Functional Mater.*, vol. 26, pp. 36–43, 2016.
- [8] T.-H. Lin *et al.*, "Enhanced light emission in vertical-structured GaN-based light-emitting diodes with trench etching and arrayed p-electrodes," *Solid-State Electron.*, vol. 107, pp. 30–34, 2015.
- [9] T. Min-An *et al.*, "Efficiency enhancement and beam shaping of GaN-InGaN vertical-injection light-emitting diodes via high-aspect-ratio nanorod arrays," *IEEE Photon. Technol. Lett.*, vol. 21, no. 4, pp. 257–259, Feb. 2009.
- [10] G. Tan, Y. Huang, M.-C. Li, S.-L. Lee, and S.-T. Wu, "High dynamic range liquid crystal displays with a mini-LED backlight," *Opt. Exp.*, vol. 26, pp. 16572–16584, 2018.
- [11] N. L. Ploch *et al.*, "Effective thermal management in ultraviolet light-emitting diodes with micro-LED arrays," *IEEE Trans. Electron Devices*, vol. 60, no. 2, pp. 782–786, Feb. 2013.
- [12] G. Christian *et al.*, "GaN-based micro-LED arrays on flexible substrates for optical cochlear implants," *J. Phys. D, Appl. Phys.*, vol. 47, 2014, Art. no. 205401.
- [13] R. Smith, B. Liu, J. Bai, and T. Wang, "Hybrid III-Nitride/Organic semiconductor nanostructure with high efficiency nonradiative energy transfer for white light emitters," *Nano Lett.*, vol. 13, pp. 3042–3047, 2013.

- [14] M. A. Moram and M. E. Vickers, "X-ray diffraction of III-nitrides," *Rep. Progress Phys.*, vol. 72, 2009, Art. no. 036502.
- [15] P. Tian *et al.*, "Size-dependent efficiency and efficiency droop of blue InGaN micro-light emitting diodes," *Appl. Phys. Lett.*, vol. 101, 2012, Art. no. 231110.
- [16] T. Zhi, T. Tao, B. Liu, Z. Xie, P. Chen, and R. Zhang, "Reverse leakage current characteristics of GaN/InGaN multiple quantum-wells blue and green light-emitting diodes," *IEEE Photon. J.*, vol. 8, no. 5, 2016, Art. no. 1601606.
- [17] T. Zhi *et al.*, "Asymmetric tunneling model of forward leakage current in GaN/InGaN light emitting diodes," *AIP Adv.*, vol. 5, 2015, Art. no. 087151.
- [18] M. Xiao-Fan *et al.*, "Fabrication and characterization of a GaN-Based 320 × 256 Micro-LED array*," *Chin. Phys. Lett.*, vol. 34, 2017, Art. no. 118102.
- [19] K. R. Son, B. R. Lee, and T. G. Kim, "Improved optical and electrical properties of GaN-based micro light-emitting diode arrays," *Current Appl. Phys.*, vol. 18, pp. S8–S13, 2018.
- [20] E. Xie *et al.*, "Design, fabrication, and application of GaN-Based micro-LED arrays with individual addressing by N-electrodes," *IEEE Photon. J.*, vol. 9, no. 6, 2017, Art. no. 7907811.
- [21] J. Cho, E. F. Schubert, and J. K. Kim, "Efficiency droop in light-emitting diodes: Challenges and countermeasures," *Laser Photon. Rev.*, vol. 7, pp. 408–421, 2013.
- [22] J. Iveland, L. Martinelli, J. Peretti, J. S. Speck, and C. Weisbuch, "Direct measurement of auger electrons emitted from a semiconductor light-emitting diode under electrical injection: Identification of the dominant mechanism for efficiency droop," *Phys. Rev. Lett.*, vol. 110, 2013, Art. no. 177406.
- [23] Z. Gong *et al.*, "Size-dependent light output, spectral shift, and self-heating of 400 nm InGaN light-emitting diodes," *J. Appl. Phys.*, vol. 107, 2010, Art. no. 013103.